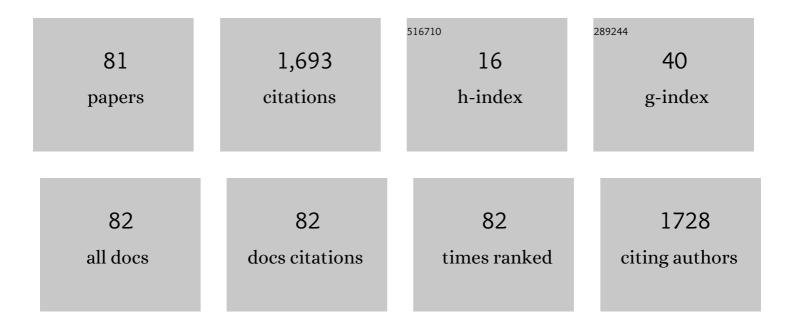
Michael L Denton

List of Publications by Year in descending order

Source: https://exaly.com/author-pdf/8818782/publications.pdf Version: 2024-02-01



#	Article	IF	CITATIONS
1	Determination of cell number in monolayer cultures. Analytical Biochemistry, 1986, 159, 109-113.	2.4	600
2	Apoptosis: definition, mechanisms, and relevance to disease. American Journal of Medicine, 1999, 107, 489-506.	1.5	270
3	The RNA polymerase I transcription factor UBF is a sequence-tolerant HMG-box protein that can recognize structured nucleic acids. Nucleic Acids Research, 1994, 22, 2651-2657.	14.5	101
4	The RNA polymerase I transactivator upstream binding factor requires its dimerization domain and high-mobility-group (HMG) box 1 to bend, wrap, and positively supercoil enhancer DNA Molecular and Cellular Biology, 1994, 14, 6476-6488.	2.3	89
5	Stimulated Raman photoacoustic imaging. Proceedings of the National Academy of Sciences of the United States of America, 2010, 107, 20335-20339.	7.1	66
6	Assessment of tissue heating under tunable near-infrared radiation. Journal of Biomedical Optics, 2014, 19, 070501.	2.6	55
7	Damage Thresholds for Exposure to NIR and Blue Lasers in an In Vitro RPE Cell System. , 2006, 47, 3065.		39
8	Histone Acetyltransferase and Protein Kinase Activities Copurify with a Putative <i>Xenopus</i> RNA Polymerase I Holoenzyme Self-Sufficient for Promoter-Dependent Transcription. Molecular and Cellular Biology, 1999, 19, 796-806.	2.3	38
9	Gene promoter of apoptosis inhibitory protein IAP2: identification of enhancer elements and activation by severe hypoxia. Biochemical Journal, 2002, 364, 413-421.	3.7	37
10	Polygalacturonase from Sitophilus oryzae: Possible horizontal transfer of a pectinase gene from fungi to weevils. Journal of Insect Science, 2003, 3, 1-9.	0.9	36
11	Spatially correlated microthermography maps threshold temperature in laser-induced damage. Journal of Biomedical Optics, 2011, 16, 036003.	2.6	36
12	Polygalacturonase from Sitophilus oryzae: Possible horizontal transfer of a pectinase gene from fungi to weevils. Journal of Insect Science, 2003, 3, 24.	1.5	32
13	Stimulated Raman scattering: old physics, new applications. Journal of Modern Optics, 2009, 56, 1970-1973.	1.3	30
14	In vitro model that approximates retinal damage threshold trends. Journal of Biomedical Optics, 2008, 13, 054014.	2.6	21
15	Pectinmethylesterase from the rice weevil, Sitophilus oryzae: cDNA isolation and sequencing, genetic origin, and expression of the recombinant enzyme. Journal of Insect Science, 2005, 5, 21.	1.5	19
16	Monitoring stimulated Raman scattering with photoacoustic detection. Optics Letters, 2011, 36, 1233.	3.3	17
17	Damage thresholds for cultured retinal pigment epithelial cells exposed to lasers at 532â€,nm and 458â€,nm. Journal of Biomedical Optics, 2007, 12, 034030.	2.6	16
18	<italic>In-vitro</italic> retinal model reveals a sharp transition between laser damage mechanisms. Journal of Biomedical Optics, 2010, 15, 030512.	2.6	16

#	Article	IF	CITATIONS
19	Wavelength- and irradiance-dependent changes in intracellular nitric oxide level. Journal of Biomedical Optics, 2020, 25, 1.	2.6	14
20	Trends in melanosome microcavitation thresholds for nanosecond pulse exposures in the near infrared. Journal of Biomedical Optics, 2014, 19, 035003.	2.6	12
21	Mathematical model that describes the transition from thermal to photochemical damage in retinal pigment epithelial cell culture. Journal of Biomedical Optics, 2011, 16, 020504.	2.6	11
22	Effect of ambient temperature and intracellular pigmentation on photothermal damage rate kinetics. Journal of Biomedical Optics, 2019, 24, 1.	2.6	10
23	Maxwell's equations-based dynamic laser–tissue interaction model. Computers in Biology and Medicine, 2013, 43, 2278-2286.	7.0	9
24	Isolation and characterization of folded fragments released by Staphylococcal aureus proteinase from the non-histone chromosomal protein HMG-1. BBA - Proteins and Proteomics, 1989, 996, 125-131.	2.1	7
25	Determination of threshold average temperature for cell death in an in vitro retinal model using thermography. , 2009, , .		6
26	Chemically Specific Imaging Through Stimulated Raman Photoexcitation and Ultrasound Detection: Minireview. Australian Journal of Chemistry, 2012, 65, 260.	0.9	6
27	Hyperthermia sensitizes pigmented cells to laser damage without changing threshold damage temperature. Journal of Biomedical Optics, 2013, 18, 110501.	2.6	6
28	Continuous assessment of metabolic activity of mitochondria using resonance Raman microspectroscopy. Journal of Biophotonics, 2021, 14, e202000384.	2.3	6
29	Accurate measure of laser irradiance threshold for near-infrared photo-oxidation with a modified confocal microscope. Journal of Microscopy, 2006, 221, 164-171.	1.8	5
30	Transient absorption spectroscopy to explore cellular pathways to photobiomodulation. Journal of Photochemistry and Photobiology B: Biology, 2021, 222, 112271.	3.8	5
31	Pigmentation in NIR laser tissue damage. , 2003, , .		5
32	Detecting mineral content in turbid medium using nonlinear Raman imaging: feasibility study. Journal of Modern Optics, 2011, 58, 1914-1921.	1.3	4
33	Thermal and damage data from multiple microsecond pulse trains at 532nm in an in vitro retinal model. Proceedings of SPIE, 2014, , .	0.8	4
34	Real-time optoacoustic temperature determination on cell cultures during heat exposure: a feasibility study. International Journal of Hyperthermia, 2019, 36, 465-471.	2.5	4
35	Spatially-correlated microthermography maps threshold temperature in laser-induced damage. , 2011, ,		4
36	Pectinmethylesterase from the rice weevil, Sitophilus oryzae: cDNA isolation and sequencing, genetic origin, and expression of the recombinant enzyme. Journal of Insect Science, 2005, 5, 1-9.	0.9	3

#	Article	IF	CITATIONS
37	An in vitro model for retinal laser damage. , 2007, , .		3
38	Laser bioeffects associated with ultrafast lasers: Role of multiphoton absorption. Journal of Laser Applications, 2008, 20, 89-97.	1.7	3
39	Mammalian complex III heme dynamics studied with pump-probe spectroscopy and red light illuminations. Biomedical Optics Express, 2021, 12, 7082.	2.9	3
40	Redox reactions of cytochrome c in isolated mitochondria exposed to blue or red lasers using resonance Raman spectroscopy. , 2018, , .		3
41	Measuring cytochrome c redox state using resonance Raman spectroscopy to determine metabolic rates in electron transport chain when exposed to light. , 2019, , .		3
42	Low irradiance light exposure alters the activity of key enzymes in the mitochondrial electron transport chain. , 2020, , .		3
43	Intracellular signaling mechanisms responsive to laser-induced photochemical and thermal stress. , 2005, , .		2
44	Exâ€CARS: exotic configuration for coherent antiâ€Stokes Raman scattering microspectroscopy utilizing two laser sources. Journal of Biophotonics, 2010, 3, 653-659.	2.3	2
45	Thermal evaluation of laser exposures in anin vitroretinal model by microthermal sensing. Journal of Biomedical Optics, 2014, 19, 097003.	2.6	2
46	Nitric oxide measurements in hTERT-RPE cells and subcellular fractions exposed to low levels of red light. , 2014, , .		2
47	Evidence of thermal additivity during short laser pulses in anin vitroretinal model. , 2015, , .		2
48	Investigation of reaction mechanisms of cytochrome c and mitochondria with transient absorption spectroscopy. , 2019, , .		2
49	Damage integral and other predictive formulas for nonisothermal heating during laser exposure. Journal of Biomedical Optics, 2022, 27, .	2.6	2
50	<title>Evidence for excitation of fluorescence in RPE melanin by multiphoton absorption</title> . , 2002, 4617, 172.		1
51	<title>Hydrogen peroxide production in cultured RPE cells exposed to near-infrared lasers</title> . , 2002, 4617, 150.		1
52	<title>Cytotoxicity in cultured RPE: a comparative study between continuous-wave and mode-locked
lasers</title> . , 2002, 4617, 156.		1
53	Melanin and the cellular effects of ultrashort-pulse, near-infrared laser radiation. , 2003, 4961, 97.		1
54	Microcavitation and spot size dependence for damage of artificially pigmented <code>hTERT-RPE1</code> cells. , 2004, , \cdot		1

#	Article	IF	CITATIONS
55	Photo-oxidation from mode-locked laser exposure to hTERT-RPE1 cells. , 2004, , .		1
56	Photochemical damage from chronic 458-nm laser exposures in an artificially pigmented hTERT-RPE1 cell line. , 2006, , .		1
57	Femtosecond light interaction with skin: Microspectroscopy of light-induced changes in collagen matrix. , 2008, , .		1
58	An in vitro corneal model with a laser damage threshold at 2 μm that is similar to that in the rabbit. , 2008, , .		1
59	Real-time monitoring of chemical and structural changes induced by light irradiation of cells and tissues. Proceedings of SPIE, 2008, , .	0.8	1
60	Correlating measured transient temperature rises with damage rate processes in cultured cells. Proceedings of SPIE, 2017, , .	0.8	1
61	Photon absorption in the mitochondria: Potential immediate and early events associated with photobiomodulation. , 2019, , .		1
62	Characterizing temperature-dependent photo-oxidation to explain the abrupt transition from thermal to non-thermal laser damage mechanisms at 413 nm. , 2011, , .		1
63	Novel approach to elucidate the nature of photomodulation therapy. , 2018, , .		1
64	A fluorescence-based approach to probing the immediate/early molecular mechanisms of photobiomodulation in vitro. , 2019, , .		1
65	Nonlinear optical characterization of retinal molecules. , 2003, , .		0
66	Detection of 2-photon oxidation from a NIR laser using confocal microscopy. , 2006, , .		0
67	Role of superoxide dismutase in the photochemical response of cultured RPE cells to laser exposure at 413 nm. , 2008, , .		Ο
68	Raman microspectroscopy of retinal pigment epithelium cells: real-time imaging the effects of photooxidative stress. , 2009, , .		0
69	A Computer-Based Model for Studying the Effects of Lasers on the Retina. , 2010, , .		Ο
70	Chemically-Specific Photoacoustic Imaging using Vibrational Raman Excitation. , 2011, , .		0
71	Stimulated Raman imaging with ultrasound detection. Proceedings of SPIE, 2011, , .	0.8	0
72	Characterizing temperature-dependent photo-oxidation to explain the abrupt transition from thermal to non-thermal laser damage mechanisms at 413 nm. Proceedings of SPIE, 2011, , .	0.8	0

#	Article	IF	CITATIONS
73	Discovery of photochemical damage mechanisms using <i>in vitro</i> and <i>in silico</i> models. Proceedings of SPIE, 2013, , .	0.8	0
74	Photothermal damage is correlated to the delivery rate of time-integrated temperature. Proceedings of SPIE, 2016, , .	0.8	0
75	Raman microspectroscopy of melanosomes in RPE cells: The effect of light irradiation. , 2008, , .		0
76	Stimulated Raman Photoacoustic Imaging. , 2010, , .		0
77	Towards Deep-Tissue Imaging: Optimizing the Excitation Wavelength. , 2014, , .		0
78	Femtosecond transient absorption spectroscopy to study the effects of low irradiance light on cytochrome c and cytochrome c reductase. , 2020, , .		0
79	Effects of specific inhibitors and low irradiance visible light on the redox cycling of cytochrome c in isolated mitochondria using resonance Raman spectroscopy. , 2020, , .		0
80	Distinguishing photothermal from photochemical damage processes at 447 nm. , 2022, , .		0
81	Near infrared laser exposure enhancement of cytochrome c oxidase enzyme activity does not exhibit irradiance reciprocity. , 2022, , .		0